NANO LETTERS

pubs.acs.org/NanoLett

Trapping and Sensing 10 nm Metal Nanoparticles Using Plasmonic Dipole Antennas

Weihua Zhang,* Lina Huang, Christian Santschi, and Olivier J. F. Martin*

Nanophotonics and Metrology Laboratory, Swiss Federal Institute of Technology Lausanne (EPFL), 1015 Lausanne, Switzerland

ABSTRACT The optical trapping of Au nanoparticles with dimensions as small as 10 nm in the gap of plasmonic dipole antennas is demonstrated. Single nanoparticle trapping events are recorded in real time by monitoring the Rayleigh scattering spectra of individual plasmonic antennas. Numerical simulations are also performed to interpret the experimental results, indicating the possibility to trap nanoparticles only a few nanometers in size. This work unveils the potential associated with the integration of plasmonic trapping with localized surface plasmon resonance based sensing techniques, in order to deliver analyte to specific, highly sensitive regions ("hot spots").

KEYWORDS Localized surface plasmon resonance, plasmonic dipole antennas, optical trapping, nanosensors

Optical trapping, as a noninvasive manipulation method, has been extensively investigated and implemented in life sciences.[1,2] Using conventional far-field techniques, micrometric dielectric particles or living cells can be trapped and manipulated, while trapping nanoparticles still remains a challenging task for the following two reasons: first, prohibitively high laser power is needed to create trapping forces large enough to overcome the Brownian motion; second, there is lack of real-time techniques for detecting the trapping events of such small particles, especially nonfluorescent nanoparticles.

Plasmonic nanostructures, however, can naturally overcome these two difficulties thanks to their capability to localize and enhance light in their near-field $\mathbf{E}$.[3−5] For a particle much smaller than the trapping light wavelength, the trapping force is proportional to the gradient of $|\mathbf{E}|^2$.[6] In the case of plasmonic structures, like for example thin metal films, metal patches, and sharp metal tips, the electric field can be enhanced and spatially localized in an area much smaller than the diffraction limit.[7] As a consequence, for similar illumination intensity, these structures generate much larger gradient forces than in the case of far-field trapping. Recently, plasmonic trapping has indeed been demonstrated experimentally and cells as well as micrometric dielectric beads have been successfully trapped using plasmonic structures with an illumination intensity much lower than that for far-field trapping.[8] Furthermore, plasmonic trapping can be easily integrated into microfluidic platforms, since it does not require a bulky and sophisticated external optical arrangement.[9] These merits offer great application potential for plasmonic trapping in the field of chemical and biosensing.

Among the huge variety of plasmonic structures that have been demonstrated in the past few years, the plasmonic dipole antenna—a pair of metal nanorods spaced by a nanometric gap—provides a very appealing choice for trapping nanoparticles. Recent studies have shown that using plasmonic dipole antennas, the electric field can be localized in the nanogap leading to a field enhancement of 2 orders of magnitude at the resonance frequency.[10−12] Moreover, the resonance frequency of plasmonic dipole antennas can be tuned to a desired value by varying the antenna length or gap size, providing additional design flexibility.[13] While the emphasis of the present publication is on trapping nanoscopic objects in the gap of the antenna, let us mention that microscopic cells have been trapped using the field generated by the whole plasmonic antenna by Righini et al.[14]

In addition to an enhanced trapping force, a plasmonic antenna can also be used to monitor in real time the trapping events from nonfluorescent nanoparticles, including particles as small as 10 nm. Actually, there is still today a lack of rapid and noninvasive methods for the detection of small nonfluorescent nanoparticles, although this detection is important for many practical applications. To the best of our knowledge, only interferometric methods are capable of detecting such small nonfluorescent nanoparticles.[15,16] Unfortunately, these methods are not suitable for near-field trapping experiments as the presence of the plasmonic trapping structures interferes with the signal of the nanoparticles. However, localized surface plasmon resonance (LSPR) sensors based on plasmonic antennas can circumvent this difficulty. Indeed, recent studies have shown that

* Correspondence to Weihua Zhang (weihua.zhang@epfl.ch) and Olivier J. F. Martin (Olivier.martin@epfl.ch).

Received for review: 12/16/2009
Published on Web: 02/12/2010

DOI: 10.1021/nl904168f | *Nano Lett.* **2010,** *10,* 1006–1011

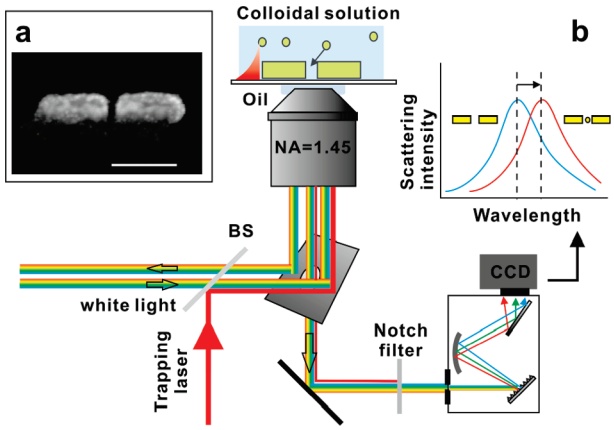

FIGURE 1. (a) SEM image of a typical nanofabricated antenna with a 10 nm gap. The scale bar is 100 nm. (b) Schematic drawing of the experimental setup. Trapping events can be directly monitored using the Rayleigh scattering spectra of the individual antennas.

the resonance frequency of a plasmonic antenna is extremely sensitive to external perturbations in its gap.[17] Especially, when the gap is only a few nanometers, a slight change of dielectric constant in the gap can induce a significant resonance shift.[18] The trapping of individual nanoparticles can therefore be monitored in real time by recording the resonance frequency of the antenna.

In this work, inspired by these ideas, Au nanoparticles are trapped using nanofabricated plasmonic dipole antennas and the trapping events are detected in real time. Two-dimensional dipole antenna arrays were fabricated using e-beam lithography with a ±5 nm precision.[19] Figure 1a shows the SEM image of a typical plasmonic antenna. The length and gap sizes of the antennas are modified individually over the array. Figure 1b sketches the optical setup which is basically a total internal reflection microscope. An oil immersion objective with a 1.45 N.A. (PLAPON 60xO TIRFM, Olympus) was used to create the evanescent wave for both trapping and characterization. An 808 nm laser (MDL-H-808, Changchun New Industries Optoelectronics Tech Co.) was injected into the outer part of the objective and then focused on the back-focal plane to create an evenly distributed evanescent field to excite the antennas. The laser power reaching the sample was 0.8 W, distributed on an area of approximately 20 × 20 μm^2, equivalent to a 2 mW laser focused onto a 1 μm^2 spot, corresponding to the power density customarily used in life sciences for laser-scanning confocal microscopy. In order to monitor the Rayleigh scattering spectra of the antennas, a white light beam was also coupled into the system with a beam splitter (BS) through the same optical path as the trapping laser. An imaging spectrometer (Shamrock SR-303i, Andor) equipped with a charge-coupled device (CCD, iDus 401BRDD, Andor) was used to record the scattering spectra of individual nanoantennas.[19,20] Typically, five or six individual antennas with a gap size from 5 to 30 nm were measured simultaneously in one experiment. A notch filter at 800 nm (Semrock) was used to block the backscattered light of the trapping laser. Au colloids with 10 or 20 nm diameters were used in this work (Sigma-Aldrich). The colloids were diluted into deionized water, with concentrations in the range between 0.1 and 1 μm^{-3}.

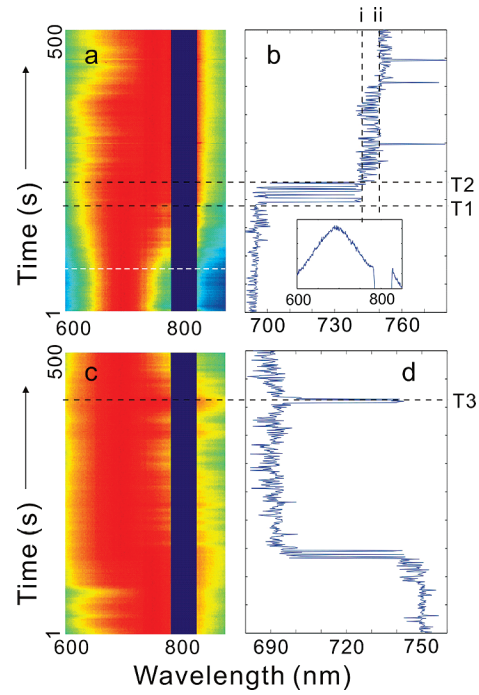

FIGURE 2. Plasmonic trapping of a 20 nm Au particle. The arm length and gap size, of the antenna are 80 nm and 25 nm, respectively. (a) Waterfall plot for 500 normalized Rayleigh scattering spectra of the antenna collected continuously; the trapping laser was on during the measurement. (b) Resonance peak wavelength of the spectra in panel a as a function of time. The inset in (b) reveals a typical Rayleigh scattering spectrum (measured along the white dashed line in panel a). The resonance frequencies used in this paper correspond to the peak wavelengths of the Rayleigh scattering spectra. (c) Waterfall plot for 500 Rayleigh scattering spectra of the antenna collected continuously while the trapping laser was off. (d) Resonance peak wavelength of the spectra in panel c as a function of the collection time. The obscured stripes in panels a and c are caused by the notch filter at 800 nm.

The measurements were performed in the following way. First, the spectra of the antennas in deionized water without Au nanoparticles were measured to ensure a clean and stable system. The trapping laser was turned on for that reference experiment. Then, Au nanoparticles were added and 500 scattering spectra were recorded continuously. Each exposure lasted for 0.3 s and was repeated every 1 s. After that, the trapping laser was turned off and another 500 spectra were recorded in order to check whether the trapped particle could be released. The measurements for each type of antenna and particle were repeated twice.

A typical experimental result is shown in Figure 2. This experiment used an antenna with a 25 nm gap and 20 nm Au nanoparticles. The peak wavelength as a function of time exhibits a characteristic stepwise behavior, as shown in Figure 2b. At the earliest stage, the resonance wavelength was constant at approximately 690 nm, and then exhibited

DOI: 10.1021/nl904168f | *Nano Lett.* **2010,** *10,* 1006–1011

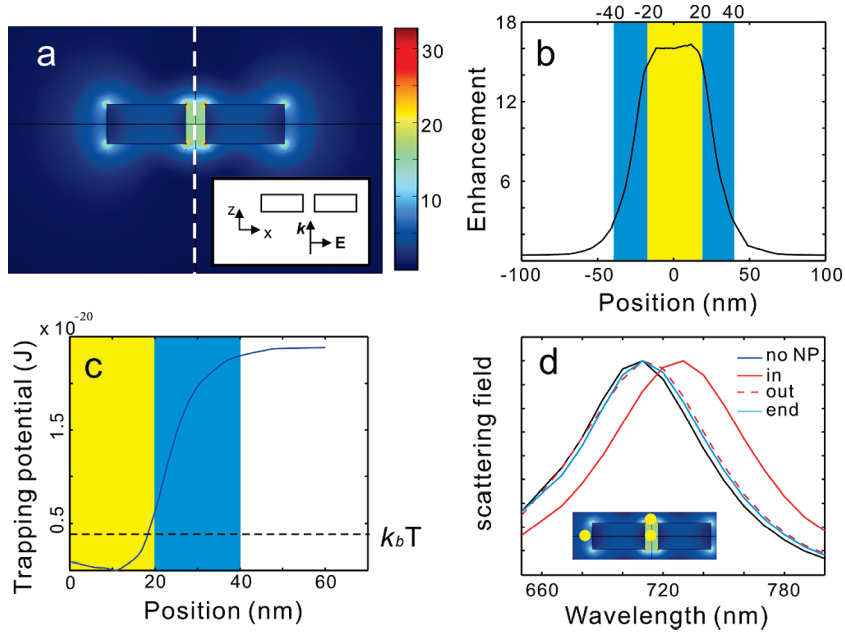

FIGURE 3. (a) Computed electric field amplitude scattered by an antenna with 80 nm arm and 25 nm gap. The inset shows the model configuration. (b) Profile of the electric field enhancement along the dashed line in (a); the origin indicates the center point of the antenna. (c) Trapping potential created by the localized electric field. The potential well exhibits a steep wall at the edge of the nanogap. (d) Rayleigh scattering spectra of the same antenna with a 20 nm nanoparticles at different locations. The black curve corresponds to the antenna without a particle; the blue curve corresponds to a nanoparticles at the antenna extremity; the red curves correspond to a nanoparticles inside (solid line) and outside (dashed line) the antenna gap. In the simulation, the distance between the particle and the antenna wall is 2.5 nm.

a sudden red shift of 50 nm at the time T1, indicating that a trapping event occurred in the antenna gap, Figure 2b. After the instant T2, the resonance frequency became stable at approximately 740 nm. However, in the period between T1 and T2, the peak wavelength oscillated between 690 and 740 nm, implying that the nanoparticle had not completely entered the gap and was swinging back and forth between two states, namely, inside and outside the gap. This phenomenon will be discussed later with the help of a numerical model.

To ensure that the red shift can be attributed to optical forces, measurements were performed with the trapping laser switched off soon after the first part of the measurement. The results are shown in Figure panels c and d of 2. After approximately 1.5 min, the Rayleigh scattering returned back to its original profile, excluding the possibility that the particle remained stuck in the gap by surface forces. In fact, during the measurement, another 50 nm red shift was also observed, at instant T3 in Figure 2d, but it only lasted for a few seconds, indicating that without optical trapping forces, the particle will not stay inside the gap, although it might make a short excursion in it. This provides direct evidence that the long lasting resonance red shift in Figure 2, panels a and b, was caused by optical trapping. Moreover, the magnitude of the shift at T3 is the same as that at T1. This implies that the trapping event observed at T1 was indeed a single particle event, not caused by several nanoparticles.

Another interesting observation in Figure 2b is the second resonance frequency jump (between i and ii) of approximately 10 nm, much smaller than the first one (approximately 50 nm). This can be explained by the trapping of a nanoparticle at one end of the antenna. In order to illustrate this, the field distribution of the antenna has been simulated and plotted in Figure 3a with two different numerical methods, namely, a commercial finite elements solver (Comsol Multiphysics) and Green's tensor technique.[21] In the model, the antenna is illuminated by a plane wave polarized parallel to the antenna. Figure 3 indicates that the field enhancement occurs not only in the antenna gap but also at the extremities of the antenna. Although the field enhancement at the extremities of the antenna is not as strong as that in the gap, the electric field remains well localized and the field intensity gradient is large. Hence, optical trapping may also take place at the extremities of the antenna.

Actually, we have observed the trapping of single Au nanoparticles at the extremities of an antenna in the following experiment reported in Figure 4. Discrete red-shift steps of approximately 10 nm were observed on an antenna with a 5 nm gap. Since in this case the gap of the antenna was too small to host a 20 nm particle, the trapping could only occur at the antenna extremities. Moreover, the magnitude of each resonance shift was consistent with the value of the small shift observed in Figure 2b.

To further investigate the relationship between trapping location and the resonance shift, we have calculated optical trapping forces by considering the nanoparticle as an ideal dipole. Under the dipole approximation, a lossy nanoparticle

DOI: 10.1021/nl904168f | *Nano Lett.* **2010,** *10,* 1006–1011

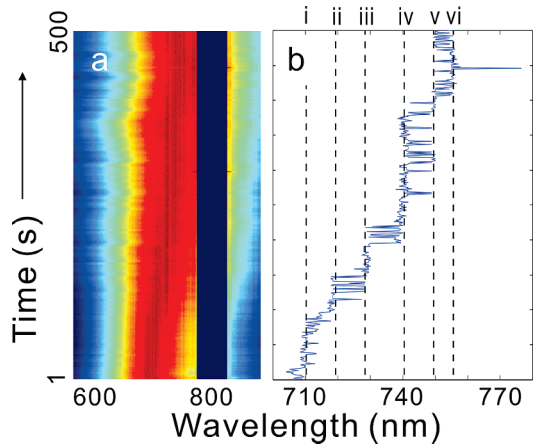

FIGURE 4. Trapping of 20 nm Au nanoparticles at the antenna extremities. The arm length and gap size of the antenna are 80 nm and 5 nm, respectively. (a) Waterfall plot of 500 Rayleigh scattering spectra of the antenna collected continuously. The trapping laser was on during the collection. (b) Peak wavelength of the spectra in (a) as the function of the collection time.

mainly experiences two types of optical forces, namely, the gradient force and the absorption force

$$\langle \mathbf{F}_{\text{grad}} \rangle = 1/2\text{Re}(\alpha)\nabla\langle |\mathbf{E}|^2 \rangle \quad (1)$$

$$\langle \mathbf{F}_{\text{abs}} \rangle = \text{Im}(\alpha)\omega\mu_0\langle \mathbf{E} \times \mathbf{H} \rangle \quad (2)$$

where α is the polarizability of the nanoparticle and the triangular brackets denote the time averages.[6] The antenna in Figure 3a is used as an example to plot the amplitude of the electric field enhancement, Figure 3b. A rapid field amplitude drop is observed in the blue area at the periphery of the antenna gap. Using eqs 1 and 2 and the experimental parameters of this work, the optical trapping potential for a 20 nm Au nanoparticle was calculated along the z axis in Figure 3a and is shown in Figure 3c. The depth of the potential well is approximately 2.4×10^{-20} J, about 6 times larger than the kinetic energy of Brownian motion which can be estimated using $k_B T = 4.1 \times 10^{-21}$ J at room temperature, where k_B is Boltzmann's constant. The field intensity at the extremities of the antenna is only a few times smaller than that in the nanogap, leading to the conclusion that the localized electric field at the extremities of the antenna is large enough to induce trapping events. It is worth mentioning that, during the reviewing period of this work, Quidant and co-workers have reported that sophisticated field calculations provide a somewhat stronger force value than those obtained from eqs 1 and 2.[22]

We have also simulated the resonance spectrum of the antenna with a 20 nm Au particle trapped at different locations, viz., at the antenna extremity or inside the gap. The results are shown in Figure 3d. When the particle is at the extremity of the antenna, the resonance shift is only a few nanometers, whereas when the particle is inside the nanogap the resonance shift reaches approximately 20 nm. This can be understood by considering that the perturbation strength of the nanoparticle, consequently the resonance shift, depends on the polarization of the nanoparticles, i.e., on the local electric field intensity. In the gap, the field enhancement is larger than that at the ends of the antenna, and therefore trapping in the antenna gap produces a significantly larger red shift than trapping at the extremities of the antenna.

In the simulation results, the resonance shift is only approximately 20 nm, smaller than the experimentally observed value. This is mainly caused by two reasons. First, a 2.5 nm distance between the particle and the antenna wall was used in the simulation in order to avoid numerical problems. However, in reality, the particle is likely to stay in close contact with the antenna, which will increase the antenna–particle interaction and shift the resonance further. Second, the nanofabricated antennas have rough walls instead of the perfectly flat surfaces used in the model. Nevertheless, the simulation results qualitatively confirm the fact that particles trapped at different locations around the antenna produce different resonance frequency shifts.

This location-dependent resonance shift is particularly well illustrated in the nanogap, as shown in Figure 3d where we simulate Rayleigh scattering spectra for antennas with a particle in the middle of the gap and just outside the gap. A substantial difference in resonance shift is observed: the shift reaches approximately 20 nm when the nanoparticle is inside the gap, whereas it is only 5 nm when the nanoparticle is just outside the gap.

This simulation also explains the aforementioned oscillating resonance frequency between times T1 and T2 in Figure 2b. In the experiment, the particle in the vicinity of the nanogap experiences two different types of forces: the random thermal force which induces the Brownian motion and the trapping force which mainly exists at the vicinity of the antenna gap. Under these two competing forces, the particle rapidly moves forth and back inside and outside the gap. Since the resonance frequency fluctuates rapidly between these two extreme wavelengths (690 nm outside the gap and 740 nm inside the gap), we can conclude that the particle oscillates through the gap before getting trapped.

After successfully trapping 20 nm Au particles, we further performed experiments using 10 nm Au particles. Because the polarizability is proportional to the volume of the particle, the trapping force decreases by a factor of 8 when the particle size changes from 20 to 10 nm. The previous simulation shows that the trapping potential is approximately 6 times that of the kinetic energy of Brownian motion, suggesting that trapping of even smaller nanoparticles might be possible after antenna optimization, namely, narrowing the nanogap. In the experiment, we observed stepwise resonance shifts—corresponding to succesive trap-

DOI: 10.1021/nl904168f | *Nano Lett.* **2010,** *10,* 1006–1011

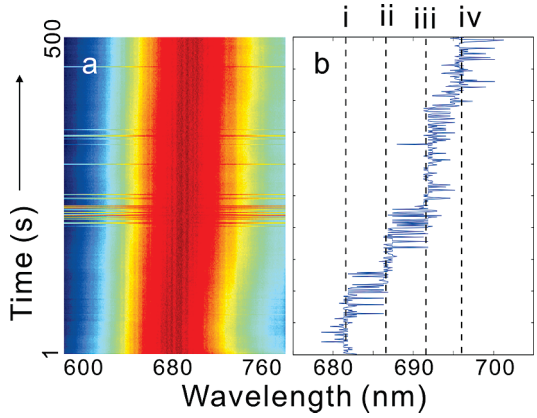

FIGURE 5. Trapping of 10 nm Au nanoparticles in the antenna gap. The arm length and gap size of the antenna are 90 nm and 15 nm, respectively. (a) Waterfall plot of 500 Rayleigh scattering spectra of the antenna collected continuously when the trapping laser was on. (b) Peak wavelength of the spectra in panel a as the function of the collection time.

ping events—using an antenna with a 15 nm gap, as shown in Figure 5. However, no trapping events were observed for antennas with a wider gap. In addition, the resonance shift is on the order of 5 nm, much smaller than that in the case of a 20 nm particle. This can be explained by the much smaller polarizability of the 10 nm particles compared to the 20 nm one.

We believe that single-molecule trapping and sensing can be achieved with a plasmonic dipole antenna by further optimizing the experimental parameters. In the calculations, the field amplitude enhancement is approximately 16 in the gap, much smaller than the predicted values in previous works.[13] Actually, the field enhancement in the antenna gap may be increased by narrowing the gap, which is indeed experimentally possible. Furthermore, recent studies in surface-enhanced Raman spectroscopy (SERS) and tip-enhanced Raman spectroscopy show that nanometric roughness can also significantly increase the local field.[23,24] On the basis of these arguments, single molecule trapping can be expected in the near future.

In the field of plasmonic trapping, an important issue currently under debate is how to exclude trapping contributions from heat-induced convection associated with light absorption in the metals. Plasmonic heating represents an important issue, which has been investigated—and even implemented—in the field of LSPR-based applications.[25−27] In the present work, we can exclude contributions associated with convection by taking advantage of multichannel detection. As aforementioned, an approximately 20 × 20 μm^2 area is illuminated and five or six antennas with different geometrical parameters—consequently, with different resonance shift—are monitored simultaneously. However, only the antennas with a 15 nm gap can trap the 10 nm nanoparticles. This is consistent with the simulation result that a narrow gap is needed to generate a lager enough field enhancement in order to trap a 10 nm particle. If it were heating-induced convection that brought the particles to the antennas, nanoparticles would accumulate on the whole illuminated area (i.e., on every antenna) and, consequently, a red shift would always be observed on each antenna. However, this was not the case in the experiments, in which only a few antennas exhibited a stepwise red shift, while the resonance of most antennas remained constant.

The absence of convection-induced particle accumulation in this work can be explained by the very low antenna density, with one nanoscale antenna in a 3 × 3 μm^2 area, and the very low laser power density. For these reasons, the total amount of heating and, consequently the convection, are negligible.

Finally, let us note that delivering the analyte specifically to the active site of a nanoscale device is an unresolved issue, for which this work might represent a step toward an appropriate solution. Today, single-molecule surfaced-enhanced Raman scattering (SERS) at individual "hot spots" has become an a very widespread technique in the laboratory,[28,29] and ultrasensitive LSPR-based sensing schemes have been proposed.[17] However, due to the dimension mismatch between the current microsample delivery techniques, i.e., microfluidics, and antenna-based sensors, it is extremely difficult to efficiently deliver a trace amount of analyte to the "hot spots" of the nanosensor. The technique developed in this work provides a strategy to address this issue. For example, recent work reported by Kall and collaborators has shown the possibility to combine optical trapping with SERS.[30] We believe that the integration of trapping with previously demonstrated sensing techniques will lead to the next generation of ultrasensitive sensing devices based on individual plasmonic nanostructures.

In summary, we have successfully trapped 10 nm Au nanoparticles using nanofabricated plasmonic dipole antennas. Single nanoparticle trapping events were recorded in real time by monitoring the Rayleigh scattering spectra of individual plasmonic antennas. Numerical simulations were also performed to interpret the experimental results, indicating the possibility to trap nanoparticles only a few nanometer in size. Moreover, this work unveils the potential associated to the integration of plasmonic trapping with LSPR-based sensing techniques, in order to deliver analyte to specific, highly sensitive regions ("hot spots").

Acknowledgment. We thank Dr. H. Fischer for his efforts in the preliminary stage of this project. This work was supported by the EPFL-STI seed fund and the Swiss National Science Foundation (Grant 200021-113735).

REFERENCES AND NOTES

(1) Ashkin, A. Acceleration and trapping of particles by radiation pressure. *Phys. Rev. Lett.* **1970**, *24*, 156–159.
(2) Grier, D. G. A revolution in optical manipulation. *Nature* **2003**, *424*, 810–816.
(3) Novotny, L.; Bian, R. X.; Xie, X. S. Theory of nanometric optical tweezers. *Phys. Rev. Lett.* **1997**, *79*, 645–648.

DOI: 10.1021/nl904168f | *Nano Lett.* **2010,** *10,* 1006–1011

(4) Quidant, R.; Girard, C. Surface-plasmon-based optical manipulation. *Laser Photonics Rev.* **2008**, *2*, 47–57.
(5) Xu, H. X.; Kall, M. Surface-plasmon-enhanced optical forces in silver nanoaggregates. *Phys. Rev. Lett.* **2002**, *89*, 246802.
(6) Novotny, L.; Hecht, B. *Principles of nano-optics*; Cambridge University Press: New York, 2006.
(7) Kottmann, J. P.; Martin, O. J. F.; Smith, D. R.; Schultz, S. Non-regularly shaped plasmon resonant nanoparticle as localized light source for near-field microscopy. *J. Microsc. (Oxford, U.K.)* **2002**, *202*, 60–65.
(8) Righini, M.; Volpe, G.; Girard, C.; Petrov, D.; Quidant, R. Surface plasmon optical tweezers: Tunable optical manipulation in the femtonewton range. *Phys. Rev. Lett.* **2008**, *100*, 186804.
(9) Huang, L.; Maerkl, S. J.; Martin, O. J. F. Integration of plasmonic trapping in a microfluidic environment. *Opt. Express* **2009**, *17*, 6018–6024.
(10) Muhlschlegel, P.; Eisler, H. J.; Martin, O. J. F.; Hecht, B.; Pohl, D. W. Resonant optical antennas. *Science* **2005**, *308*, 1607–1609.
(11) Xu, H. X.; Bjerneld, E. J.; Kall, M.; Borjesson, L. Spectroscopy of single hemoglobin molecules by surface enhanced Raman scattering. *Phys. Rev. Lett.* **1999**, *83*, 4357–4360.
(12) Xu, H. X.; Aizpurua, J.; Kall, M.; Apell, P. Electromagnetic contributions to single-molecule sensitivity in surface-enhanced Raman scattering. *Phys. Rev. E* **2000**, *62*, 4318–4324.
(13) Fischer, H.; Martin, O. J. F. Engineering the optical response of plasmonic nanoantennas. *Opt. Express* **2008**, *16*, 9144–9154.
(14) Righini, M. Nano-optical Trapping of Rayleigh Particles and Escherichia coli Bacteria with Resonant Optical Antennas. *Nano Lett.* **2009**, *9*, 3387–3391.
(15) Arbouet, A. Direct measurement of the single-metal-cluster optical absorption. *Phys. Rev. Lett.* **2004**, *93*, 127401.
(16) Lindfors, K.; Kalkbrenner, T.; Stoller, P.; Sandoghdar, V. Detection and spectroscopy of gold nanoparticles using supercontinuum white light confocal microscopy. *Phys. Rev. Lett.* **2004**, *93*, No. 037401.
(17) Jain, P. K.; El-Sayed, M. A. Noble Metal Nanoparticle Pairs: Effect of Medium for Enhanced Nanosensing. *Nano Lett.* **2008**, *8*, 4347–4352.
(18) Alu, A.; Engheta, N. Tuning the scattering response of optical nanoantennas with nanocircuit loads. *Nat. Photonics* **2008**, *2*, 307–310.
(19) Zhang, W. H.; Fischer, H.; Schmid, T.; Zenobi, R.; Martin, O. J. F. Mode-selective surface-enhanced Raman spectroscopy using nanofabricated plasmonic dipole antennas. *J. Phys. Chem. C* **2009**, *103*, 14672–14675.
(20) Sonnichsen, C. Spectroscopy of single metallic nanoparticles using total internal reflection microscopy. *Appl. Phys. Lett.* **2000**, *77*, 2949–2951.
(21) Martin, O. J. F.; Dereux, A.; Girard, C. Iterative scheme for compluting exactly the total field propagating in dielectric structures of arbitrary shape. *J. Opt. Soc. Am. A* **1994**, *11*, 1073–1080.
(22) Juan, M. L.; Gordon, R.; Pang, Y. J.; Eftekhari, F.; Quidant, R. Self-induced back-action optical trapping of dielectric nanoparticles. *Nat. Phys.* **2009**, *5*, 915–919.
(23) Jackson, J. B.; Halas, N. J. Surface-enhanced Raman scattering on tunable plasmonic nanoparticle substrates. *Proc. Natl. Acad. Sci. U.S.A.* **2004**, *101*, 17930–17935.
(24) Zhang, W. H. Nanoscale roughness on metal surfaces can increase tip-enhanced Raman scattering by an order of magnitude. *Nano Lett.* **2007**, *7*, 1401–1405.
(25) Hirsch, L. R. Nanoshell-mediated near-infrared thermal therapy of tumors under magnetic resonance guidance. *Proc. Natl. Acad. Sci. U.S.A.* **2003**, *100*, 13549–13554.
(26) Zhang, W. H.; Schmid, T.; Yeo, B. S.; Zenobi, R. Near-field heating, annealing, and signal loss in tip-enhanced Raman spectroscopy. *J. Phys. Chem. C* **2008**, *112*, 2104–2108.
(27) Baffou, G.; Quidant, R.; Girard, C. Heat generation in plasmonic nanostructures: Influence of morphology. *Appl. Phys. Lett.* **2009**, *94*, 153109.
(28) Kneipp, K. Single molecule detection using surface-enhanced Raman scattering (SERS). *Phys. Rev. Lett.* **1997**, *78*, 1667–1670.
(29) Nie, S. M.; Emery, S. R. Probing single molecules and single nanoparticles by surface-enhanced Raman scattering. *Science* **1997**, *275*, 1102–1106.
(30) Svedberg, F.; Li, Z. P.; Xu, H. X.; Kall, M. Creating hot nanoparticle pairs for surface-enhanced Raman spectroscopy through optical manipulation. *Nano Lett.* **2006**, *6*, 2639–2641.

DOI: 10.1021/nl904168f | *Nano Lett.* **2010,** *10,* 1006–1011